

ENERGY AND EXERGY ANALYSIS OF AN AIR SOURCE HEAT PUMP UNDER VARIABLE AMBIENT CONDITIONS

Giedrė STRECKIENĖ, Tomas KROPAS, Rūta MIKUČIONIENĖ[✉], Rasa DŽIUGAITĖ-TUMĖNIENĖ

Department of Building Energetics, Vilnius Gediminas Technical University, Vilnius, Lithuania

Highlights:

- energy and exergy analyses are used to evaluate ASHP operation's experimental data;
- HP performance indicators are COP, COP_{Carnot} , exergy efficiency, primary energy ratio;
- $T_{out} = 0$ °C and RH = 95% are the worst conditions for the operation of ASHP.

Article History:

- received 28 March 2023
- accepted 26 September 2023

Abstract. Air source heat pumps (ASHPs) are becoming an increasingly popular heating source for buildings. The paper presents an evaluation of the experimental data from ASHP operation during the heating season in Lithuania when the problem of the evaporator's surface freezing is visible. The performance of the air-to-water heat pump is examined using energy and exergy analyses performed by a coefficient of performance (COP), COP_{Carnot} , exergy efficiency, and primary energy ratio. Analysis results show that the existing difference between the ideal and actual operation of ASHP represents the demand to improve the performance of ASHP evaporator. The actual COP was from 3.5 to 4.7 times lower than the Carnot COP. At 0 °C and 95% humidity, the ASHP's performance was least favourable, with an average exergy efficiency of 0.21 and a COP of 1.49.

Keywords: air source heat pump, thermodynamic analysis, ambient conditions, performance, exergy.

[✉]Corresponding author. E-mail: ruta.mikucioniene@vilniustech.lt

1. Introduction

Human activities and their associated impacts are deeply felt around the world. With the development of various technologies and the emergence of innovations, the climate crisis and its related consequences, the effects of which are relevant globally, are increasingly being talked about, but perhaps still not enough. The European Green Agreement (European Green Deal) was adopted in 2020, a series of European Commission policy initiatives aimed at making the European Union (EU) neutral in 2050. A plan to assess the impact will also be proposed to increase the EU's target for reduction in greenhouse gas emissions for 2030 to at least 50% and 55% compared to 1990 levels (European Commission, 2019). Concepts of sustainable development and green growth strategies cover social, economic, and environmental issues. Natural resources and independence of the points of fossil fuels are one of the Green growth strategies (Pyliavskiy et al., 2021). Energetics is one of the leading areas where it is possible and efforts are being made to reduce the impact of climate change as strongly as possible. For these reasons, the energy sector

will move away from fossil fuel energy production to renewable energy to decarbonize. Heat pumps (HPs) provide an increasingly attractive option for further decarbonization (Carroll et al., 2020; European Academies' Science Advisory Council, 2021; Lepiksaar et al., 2021). Furthermore, HPs together with other renewables are common decisions in net zero energy buildings (NZEB) (Chen, 2019).

Recently, a particularly large development of them has been observed. Such devices are increasingly used in building heating and hot water preparation systems, and air conditioning systems. Most sales in the European market are made up of air-source heat pumps (ASHPs) (EurObserv'ER, 2021; Witkowska et al., 2021). The installation of the ASHP in nearly zero-energy buildings is currently on the increase (García-Gáfaró et al., 2022). However, the performance of ASHPs and their efficiency are variable over the year and strongly depend on climatic conditions (Gupta & Irving, 2013; Kropas et al., 2022; Madonna & Bazzocchi, 2013). Winter season is especially important (Wang et al., 2021). As the outside air temperature decreases, the coefficient of performance (COP) of the ASHP also decreases, and at high relative humidity,

the evaporator heat exchanger begins to freeze, which worsens the heat exchange and increases the energy consumption of the system (Chung et al., 2019; Dincer & Rosen, 2015; Hwang & Cho, 2014; Rafati Nasr et al., 2014). Different defrosting technologies have been extensively studied (Song et al., 2018; Willem et al., 2017), however, in countries with a cold climate, this problem is still particularly relevant, and the need for further research in this area can be seen in the works of many scientists (Alva et al., 2018; Amer & Wang, 2017; Kropas et al., 2022; Rafati Nasr et al., 2014; Song et al., 2018). Improved performance of air source heat pumps can help reduce energy losses, and better understanding and improving their operating algorithms can make a strong contribution to combating climate change (Carroll et al., 2020; Willem et al., 2017).

Generally, to assess the quality of the ASHP system's process, the energy efficiency is calculated using the principles of the first law of thermodynamics (Carroll et al., 2020; Kropas et al., 2021; Wang et al., 2021). Energy conservation law expresses the balance of different forms of energy in the system affected by transformation, assesses the energy of different forms of energy passing through the system and outside, but does not assess the quality or level of that energy (Dincer & Rosen, 2013; Martinaitis, 2007; Njoku et al., 2016). Therefore, quantitative and qualitative analysis of these systems is needed.

Thermodynamic analysis that combines energy and exergy efficiency (hence the 1st and 2nd laws of thermodynamics) is often found in the literature when analysing engineering systems using HP's (Akbulut et al., 2016; Martinaitis et al., 2018; Mateu-Royo et al., 2019; Mete Ozturk et al., 2020). When evaluating the exergy efficiency of systems, one of the accepted quantities is exergy destruction (Çakir et al., 2013; Martinaitis et al., 2018; Wang et al., 2020). Which is a measure of resource degradation (Dincer & Abu-Rayash, 2020). The amount of exergy destroyed by different heat pump components isn't the same (Dong et al., 2017; Shao et al., 2021; Wang et al., 2020). Wang et al. examined air source transcritical carbon dioxide HP water heater components and found that the largest exergy destruction occurred in the evaporator, accounting for 44.04–49.22 per cent of the total. The detailed energy and exergy analyses showed that the system heating performance could be improved with the optimal charge and the evaporator needed improvement to increase the exergy efficiency (Wang et al., 2020). Çakir et al. investigated an experimental exergetic comparison of four different HP systems working under the same conditions: air to air, air to water, water to water and water to air. The ranking of the four HP types from high to low according to the mean exergy efficiencies of each one showed that the water-to-air HP has the best efficiency (30.23%), however, ranking of the four HP types from high to low according to the exergy destruction rates of them showed that air to air HP has the biggest exergy destruction (2.93 kW) compared with others. The study revealed that when air is used at the evaporator, a change in mass flow rate causes a serious increase in exergy destruction of the system (Çakir et al.,

2013). Previous studies indicate that combining energy analysis with exergy analysis offers a more comprehensive understanding of heat pumps' performance, highlighting areas for enhancement. This approach aligns with sustainability objectives as it considers both quantitative and qualitative criteria, making it a more holistic assessment method.

The objective of the study is to analyze the performance of an Air Source Heat Pump (ASHP) through thermodynamic analysis. This analysis specifically focuses on the heating period, particularly when there's a potential for the evaporator surface to freeze. Simultaneously, the intention is to examine how both the operational mode of the ASHP and the surrounding environmental parameters impact the efficiency of the unit. To achieve this goal, four distinct efficiency indicators have been selected: the widely used Coefficient of Performance (COP), along with three supplementary efficiency measures – Carnot COP, exergy efficiency, and primary energy ratio (PER). Moreover, the latter indicator also considers the primary energy consumption of the heat pump, which plays a role in evaluating the unit's sustainable operation. The study's findings highlight a growing need for a more thorough evaluation of how climate conditions affect the efficiency of air-source heat pumps, especially as they become increasingly popular for heating and providing domestic hot water in colder and temperate regions. This underscores the importance of more extensive planning in both the development and operation of such systems.

2. Methods and materials

2.1. ASHP energy and exergy analysis

The ASHP operates between low-temperature (T_L – ambient air) and high-temperature (T_H – hot water temperature) reservoirs. The energy balance for the entire HP system can be written as follows:

$$\dot{W} + \dot{Q}_L = \dot{Q}_H, \quad (1)$$

where \dot{W} denotes the work input rate into the system, \dot{Q}_L and \dot{Q}_H denote evaporator and condenser heat loads, respectively. In addition, the energy balance helps to calculate the extraction rate of heat from the environment (\dot{Q}_L).

Several typical assumptions are made to analyze the operation of ASHP: the reference state for the system is an environmental temperature that was measured; the kinetic and potential energy changes are negligible.

Concerning energy balance, the COP is used to measure the HP heating performance when it is operating in heating mode. It shows the ratio of the ASHP heat output (\dot{Q}_H) to its electrical input \dot{W} and is expressed in this way

$$COP = \frac{\text{Heat input}}{\text{Electricity input}} = \frac{\int \dot{Q}_H dt}{\int \dot{W} dt}. \quad (2)$$

The power used by the heat pump is calculated using the following expression: $\dot{W} = I \times U \times \cos \phi$. Where I is the current (from the experiment); U is the voltage, and \cos

φ is the power factor; t is the time. The heat output is obtained from:

$$\dot{Q}_H = \dot{V} \times \rho \times c_p (T_{H,in} - T_{H,out}), \quad (3)$$

where \dot{V} is the water flow rate; ρ is the water density; c_p is the specific heat capacity; $T_{H,in}$ is the temperature of the water supplied; $T_{H,out}$ is the temperature of the water returned.

The maximum COP of a heat pump cycle, which operates between the temperature limits T_L and T_H , can be expressed using the principles of the Carnot heat pump.

$$COP_{Carnot} = \frac{T_H}{T_H - T_L}. \quad (4)$$

Thus, the COP_{Carnot} shows the limit on HP performance. This indicator is lower when a greater temperature rise is required. In many real-life situations, the actual HP's COP is much lower than Carnot's value (Bonin, 2015; Rimbala et al., 2019).

If the ASHP system boundaries include the energy chain from primary energy input to the final energy input to the system, performance indicators related to the usage of renewable energy or primary energy use can be calculated. For example, the Primary Energy Ratio (PER) is defined as the ratio of the output of useful energy (energy for heating) to primary energy input (Bonin, 2015); (Malenković, 2012). Primary energy input is defined as total energy input. It includes renewable energy input and non-renewable energy input. PER may be estimated as follows:

$$PER = \frac{\text{Useful energy}}{\text{Primary energy}}. \quad (5)$$

For systems using energy from different primary sources, the primary energy factors (f_{PR}) are used. They depend on the location of the system. The current study uses Lithuanian national regulations. When the ASHP uses the electricity that is produced in different ways, f_{PR} is taken to be 2.3 (Ministry of Environment of the Republic of Lithuania, 2022, Nr. D1-281).

Exergy analysis enables the determination of the system's exergy destruction rate and the efficiency of the system or each component. The total exergy of the system is composed of four main components: physical, kinetic, potential, and chemical. This study evaluates only the physical exergy for the ASHP efficiency calculations and consists of two components: mechanical exergy (related to system pressure) and thermal exergy (related to system temperature).

The exergy balance equation of the ASHP is defined as follows:

$$\dot{E}x_{in} = \dot{E}x_{out} + \dot{L}x, \quad (6)$$

where $\dot{E}x_{in}$ is the total exergy of energy inputs and evaluates electricity input in the compressor ($\dot{E}x_{in,cm}$) and exergy of heat extracted from the environment ($\dot{E}x_{in,ev}$). Finally, exergy input is defined as $\dot{E}x_{in} = \dot{E}x_{in,cm} + \dot{E}x_{in,ev}$. The

exergy transfer rate by heat is calculated using the Carnot factor $\dot{E}x = \dot{Q} \left(1 - \frac{T_a}{T}\right)$.

The total exergy destruction rate of the entire heat pump cycle ($\dot{L}x_{total}$) can be calculated by analysing the exergy balance of the entire system or by summing the exergy destruction rates of the components (e.g. compressor (cm), condenser (cn), evaporator (ev), throttle valve (tv)):

$$\begin{aligned} \dot{L}x_{total} &= \dot{L}x_{cm} + \dot{L}x_{cn} + \dot{L}x_{ev} + \dot{L}x_{tv} = \\ &\dot{E}x_{in} - \dot{Q}_H \left(1 - \frac{T_a}{T_H}\right), \end{aligned} \quad (7)$$

where T_a is the reference environment temperature. When the ASHP works as a heating device, T_a is usually set to the temperature of the low-temperature medium and it is the same as the temperature of ambient air. In this study, the exergy destruction in the system components is not calculated.

The HP exergy efficiency during the heating mode is defined as:

$$\eta_{ex} = \frac{\dot{E}x_{out}}{\dot{E}x_{in}} = \frac{\dot{Q}_H \left(1 - \frac{T_a}{T_H}\right)}{\dot{E}x_{in}}. \quad (8)$$

In this way, it is possible to compare both the amount of exergy consumed and produced, as well as the exergy efficiency of the ASHP. In addition, the enthalpies relationship (h_{air}/h_{water}) between the ambient air parameters and hot water parameters is used to analyse the variation of the exergy efficiency. Enthalpy as a state function was selected as it represents the heat energy due to temperature and moisture in the air. The water enthalpy is calculated using the equation presented by Popiel and Wojtkowiak (1998). The enthalpy of ambient air evaluates the temperature and specific humidity of the air and is calculated as follows:

$$h_{air} = 1.006 \times t_{air} + SH_{air} (2501 + 1.86 \times t_{air}), \quad (9)$$

where t_{air} is the air temperature; SH_{air} is the air-specific humidity.

2.2. Experimental set-up and measurements

The experimental setup (see Figure 1) was made specifically for testing the ASHP operation. This experimental setup was also used and described in detail in the previous study where evaporator surface freezing has been analysed in detail (Kropas et al., 2021).

The ASHP was installed on the roof of the Faculty of Environmental Engineering at Vilnius Gediminas Technical University. The rated nominal heating capacity of the ASHP was 7 kW and the COP was 4.46 at an environment temperature of 7 °C and the temperature of the water flow from the condenser at 35 °C. The R410 was used as a working fluid.

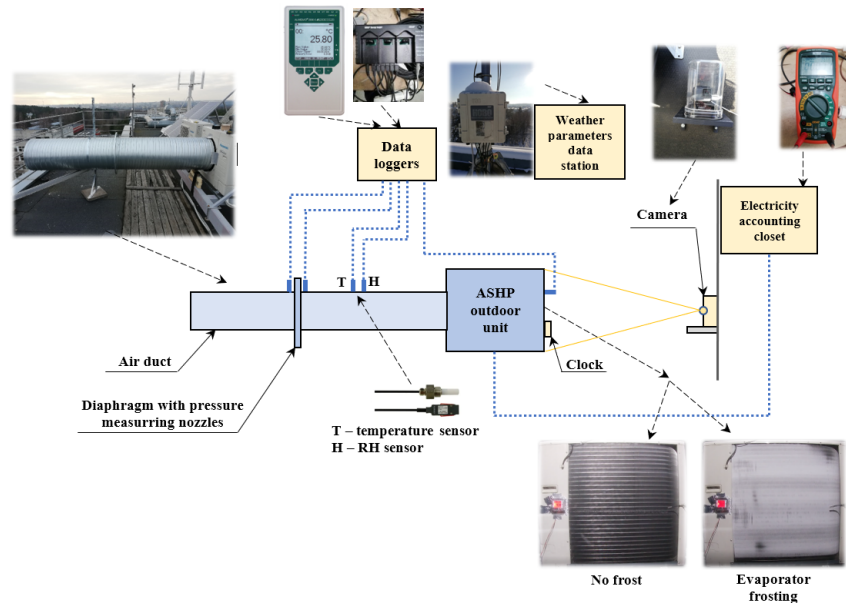


Figure 1. The schematic representation of the experimental setup

The uncertainty of the parameters measured directly is shown in Table 1.

Table 1. Characteristics of measuring equipment

Parameter	Equipment	Main characteristics
Air pressure and relative humidity (RH)	IRIS flow control diaphragm with measurement nozzles. Pressure sensors FD A602-S1K	The measurement range is ± 1250 Pa, and the RH accuracy is 2.0%
Air temperature and RH	Sensor S-THB-M002	The accuracy of the air temperature is 0.21 °C (0 to 50 °C) and the accuracy of RH is 2.5% (Protective caps for capacitive humidity sensors FHA 646 E1, 2021) (Onset, n.d.-a)
Water temperature	Temperature sensor S-TMB-M017	The accuracy is ± 0.2 °C from 0 °C to 50 °C (Onset, n.d.-b)
Water flow rate	Sensor T-MINOL-130-NL	It measures from 0.95 l/min to 83.3 l/min, and has AWWA accuracy (American Water Works Association) spec 97–103% (Onset, 2021)
Electric current	EX542 multi-meter and data-logger	Accuracy: $\pm 0.06\%$ (MultiMeter/Datalogger EX542 specification, 2021)
Power factor	Leakage clamp TRMS meter	Is used for power factor measurement. The accuracy is ± 5 digits. The range is from 0 to 1.00 (Metrel, 2021)

The actual flow rate of air was calculated based on the pressure difference measured using the IRIS-type flow control diaphragm. The data loggers were used for the storage of air and water parameters.

The air source heat pump prepared hot water, which was further supplied to the storage tank of the real operating laboratory heating system. As it was intended to simultaneously study the effect of freezing, the temperatures of the water supplied to the storage and returned to the heat pump were kept sufficiently high, ranging from 42.4 to 52.9 °C on different days, respectively. This mode of operation is chosen to simulate the operation of a real heating and hot water preparation system. The corresponding flow rates are indicated in Table 2. Next, hot water from the tank was supplied to the heating system of the laboratory premises.

The experiments mainly focused on colder weather conditions when the frost-defrost cycles of the ASHP evaporator occurred. Measurements were carried out between 29 October 2020 and 12 January 2021 and recorded every minute. During this period, the ambient air temperature ranged from -7.6 °C to 11.4 °C and the relative humidity (RH) varied from 46.3% to 97.5% (Figure 2a). Taking into account the duration of the period and the frequency of the temperatures, the environmental air temperature of around 0 °C was estimated to account for the largest proportion (i.e. 11.1%) compared to the other environmental air temperatures. When the range of air temperatures was extended from -1 °C to $+1$ °C, it accounted for 27.5% of the total temperatures for the period. Furthermore, the entire period was characterised by high RH, with 88.6% of the time having RH above 85%. All measurements were recorded every 1 minute.

3. Results and discussion

3.1. Analysis of the operating conditions

To analyse the influence of the ambient conditions on the performance of the heat pump by thermodynamic analysis, typical days with an average outdoor daily temperature $<5\text{ }^{\circ}\text{C}$, with strong diurnal variations but positive temperatures of around $0\text{ }^{\circ}\text{C}$ and around $-4\text{ }^{\circ}\text{C}$ were selected from the period considered. Details are given in Table 2 and the variation of the ambient air parameters during these days is in Figure 2. In addition, Table 2 shows the operating parameters of the ASHP: average airflow through the evaporator and the parameters of the heat transfer fluid to be prepared: flow rate, supply and return temperatures.

It was observed that evaporator freezing starts when the outdoor relative humidity reaches 88% and the air temperature drops to $3.5\text{ }^{\circ}\text{C}$ and below. The frost formation on the surface of the evaporator plates disrupts the

normal operating cycle and reduces the heat transfer ratio. When the heat exchanger frosts, an ice removal process is performed – defrosting, when the heat pump starts to run in a reverse cycle and hot freon gas melts down the ice cover.

Figure 2 shows that the RH remained high during all the days considered. The selected days are also characterised by the fact that on 31 October and 10 January, the air temperature fluctuation was relatively small compared to the selected days in November and December. The air temperature rose on December 16, but during the day it fluctuated to about $0\text{ }^{\circ}\text{C}$, leading to the formation of ice on the evaporator surface.

3.2. Energy and exergy flows in the system

In order to determine the selected indicators of the thermodynamic analysis, first of all, the corresponding values of the energy and exergy balances were found. From the

Table 2. Operating conditions of the ASHP

Date, yy/mm/dd	Temperature (t_a), $^{\circ}\text{C}$			RH, %			Air flow rate*, m^3/h	Water*		
	Average	Min	Max	Average	Min	Max		Flow rate, m^3/h	t_{supply} , $^{\circ}\text{C}$	t_{return} , $^{\circ}\text{C}$
2020 October 31	7.71	6.54	8.82	95.4	92.7	96.8	4251	1.33	52.89	49.98
2020 November 20	3.23	0.91	7.39	85.2	75.6	93.3	2250	1.34	47.75	45.81
2020 December 16	-0.14	-1.96	1.86	95.1	93.6	96.5	3630	1.32	46.35	44.20
2021 January 10	-4.23	-4.71	-3.48	92.8	89.7	94.2	4655	1.39	42.42	40.62

Note: * shows average values.

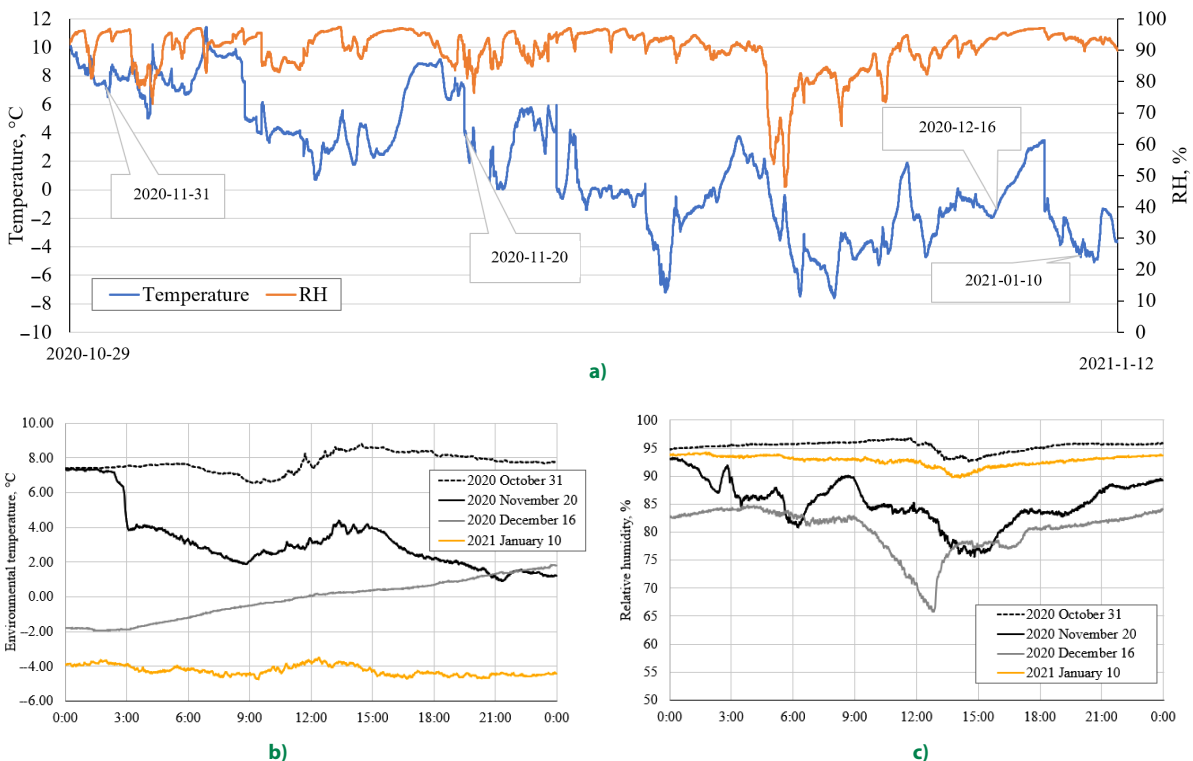


Figure 2. Environmental air parameters: a) entire measurement period; b) temperature during the selected days; c) relative humidity during the selected days

experimental data, the flow of exergy entering the heat pump is estimated, which in this case is mostly electricity, because the recalculated amount of exergy received in the evaporator from the ambient air accounted for only 1 per cent of the total exergy received. The exergy flow leaving the heat pump (Ex,out) and the destroyed exergy are also

determined. These values are presented in typical days in Figure 3. Energy balance components are also presented here, i.e. heat received from the environment, and heat given to the heated water. The electric power used in the case under consideration is relevant for both: energy and exergy balance.

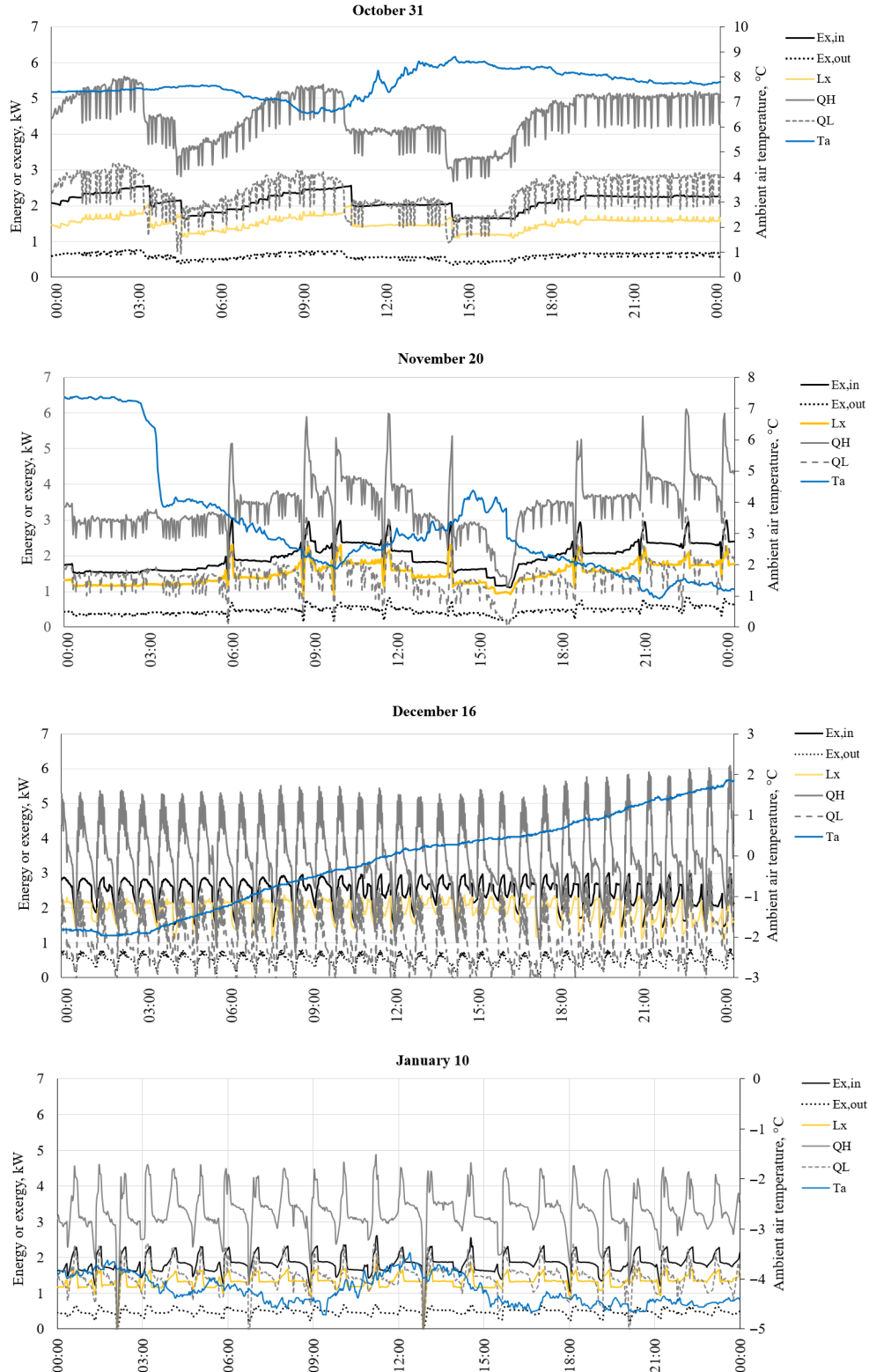


Figure 3. Components of energy and exergy balances on the respective days

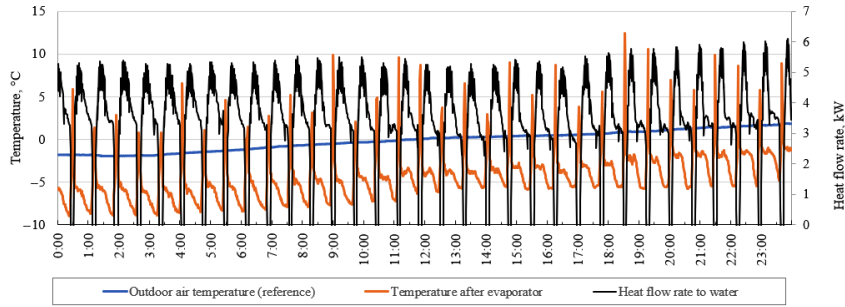


Figure 4. Temperatures before and after the evaporator, and heat flow rate to water on December 16

It can be seen from Figure 3 that the ASHP operates cyclically to prepare hot water every day. In a general trend, heat demand dictates the amount of exergy and thus energy consumed. When comparing the performance of the ASHP on different days, December 16 stands out. This period was characterized by ice formation on the evaporator surface. The ambient air temperature, the air temperature after the evaporator, and the heat flow to the water on 16 December are shown in Figure 4. 33 frost-defrost cycles were recorded on that day. The average time taken to defrost a frozen evaporator was about 5 minutes. The average defrosting time remained practically the same for the different tests and was independent of the ambient air parameters; only the cycle frequency varied.

The refrigerant in the evaporator was unable to absorb the energy needed from the air and evaporate, so the evaporation temperature had been reduced to conduct the heat exchange. Here, frequent peak elevations were observed, which were characteristic of the evaporator defrost process, when hot Freon gas was directed to the evaporator heat exchanger to melt the frost.

3.3. Evaluation of heat pump performance

The change and trends of COP and exergy efficiency indicators for the considered days are presented in Figure 5. Since on October 31, a higher hot water temperature was maintained compared to the other considered days, this had an impact on the non-dawn COP and at the same time the exergy efficiency coefficient, which was 2.11 and 0.28, respectively. In addition, the surface of the evaporator did not freeze, as the lowest air temperature recorded during the considered period was 6.45 °C, although it maintained an average of 95.4% RH. November 20 was characterized by the outdoor air temperature still positive, but falling from 7.39 to 0.91, when the average RH was around 85.2%, and more favourable frosting conditions began to form on the surface of the evaporator, as a result of which a drop in COP was observed below 1.0, and the exergy efficiency dropped to 0.11.

As can be seen from Figure 5, the most critical day is December 16, when freezing of the evaporator surface was observed practically every hour, and defrosting was also required. The COP value was often lower than 1.0 and

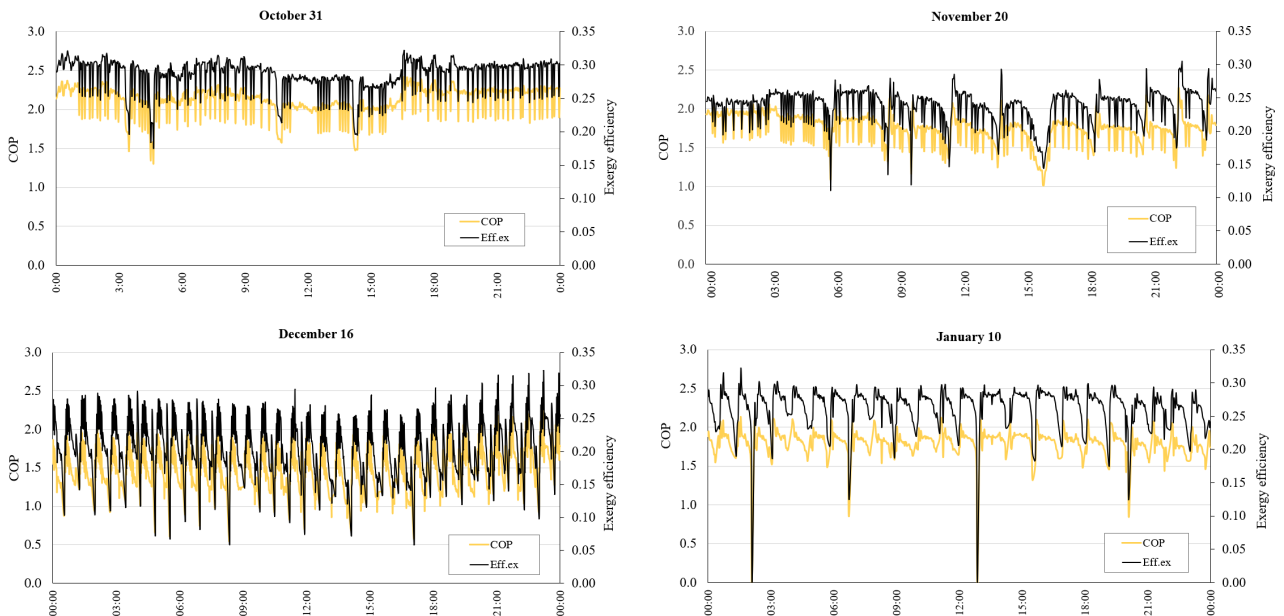


Figure 5. Variation of exergy efficiency and COP

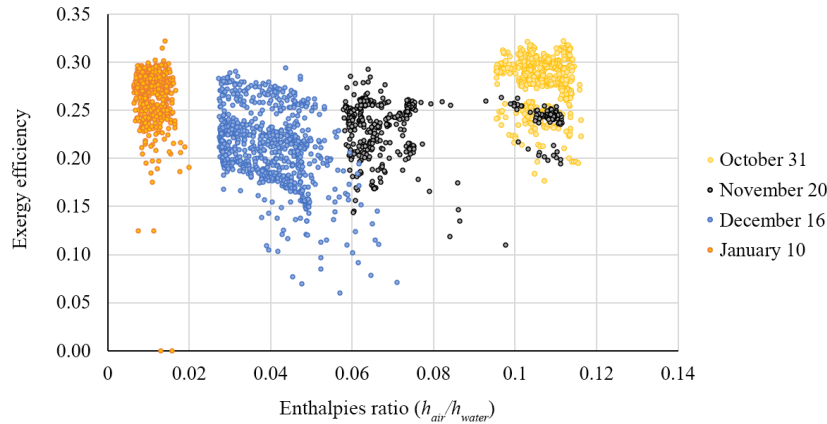


Figure 6. Dependence of exergy efficiency on enthalpy ratio (h_{air}/h_{water})

averaged only 1.49, and the average value of exergy efficiency was also the lowest compared to other days, i.e. 0.21. Freezing of the evaporator surface was also noticeable on January 10, but this phenomenon was less frequent, and the RH was lower than on December 16. During the investigation, it was found that on January 10 the average COP value was 1.82, and the average exergy coefficient value was 0.27. The temperature of the hot water produced was of additional importance to these efficiencies, it was on average 42.42 °C in the supply line, while it was higher on other days.

The enthalpy parameter was used to assess the complex influence of ambient air parameters (temperature and RH) and supply hot water parameters. The air enthalpy parameter assesses both air temperature and humidity, effectively indicating the amount of heat energy contained within the air. By combining the air enthalpy (h_{air}) ratio with the enthalpy of the supply hot water (h_{water}), the performance of the ASHP can be more universally assessed. Figure 6 shows the influence of h_{air}/h_{water} on the exergy efficiency. It can be seen that different days were characterized by a unique combination of enthalpy differences, which together influenced exergy efficiency. Since November 20 was characterized by a greater temperature change compared to other days, the exergy efficiency values during that day overlapped with both October 31 and December 16. The results of December 16 additionally show a large dispersion of the exergy efficiency and an unstable operation of the heat pump. The results of January 10 are

the least scattered due to the relatively constant temperature and RH that prevailed on that day, which can be seen together in Figure 2.

The analysis of enthalpies ratios on the exergy efficiency shows that the smallest exergy efficiencies are determined when the h_{air}/h_{water} was between 0.04 and 0.06. This indicates that for a given combination of ambient air conditions and supply hot water parameters, more frequent evaporator frost-defrost cycles are observed. Therefore, the combined influence of several parameters needs to be included to evaluate strategies to improve evaporator performance.

Summarizing the different evaluation criteria of the ASHP for the examined days, their average values are presented in Figure 7.

In addition to the already discussed COP and exergy efficiency comparison, COP_{Carnot} and PER are included. Comparing the actual COP with the COP_{Carnot} , it can be seen that the COP is reduced by a factor of 3.5 when no evaporator freezes are recorded to a factor of 4.7 (December 16) when frequent evaporator frost-defrost cycles occur. The large difference between the actual COP and COP_{Carnot} shows that the performance of the ASHP can be strongly improved in the periods considered. Accordingly, when assessing the PER indicator, the latter varied on average from 0.65 to 0.92. Naturally, this value would nearly double if the operation of the ASHP was powered by renewable energy sources. The comprehensive assessment underscores the importance of analyzing multiple

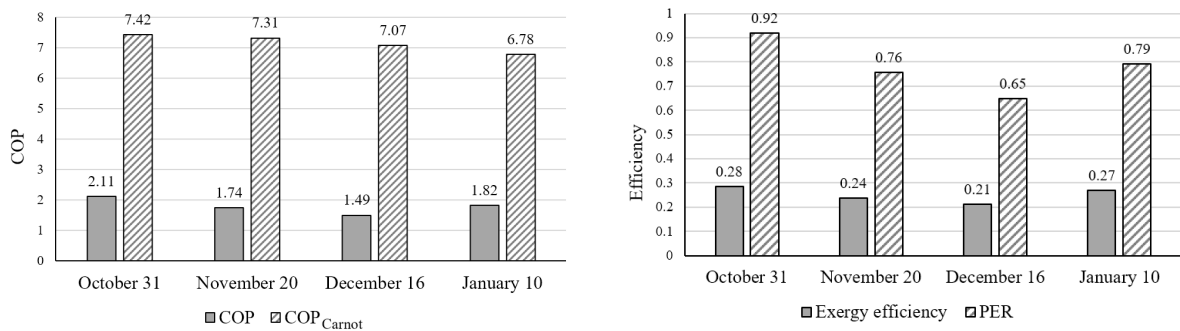


Figure 7. Comparison of heat pump COP, COP_{Carnot} , exergy efficiency and PER

performance criteria and employing indicators that encompass operating conditions, such as the enthalpy value, in a unified approach. Furthermore, the study emphasizes the necessity for a detailed analysis of the impact of frost formation on the evaporator surface itself, potential prevention strategies, and their effects on both exergy efficiency and other relevant indicators.

The quantitative and qualitative analysis of the ASHP systems, using sustainability criteria to assess environmental impacts, is essential to improve ASHP performance and promote the spread of technology in cold climate countries. Therefore, the future is planned to evaluate ASHP performance using additional indicators for assessing sustainable system development. Future efforts will involve additional simulation research to examine various operation modes of the ASHP system. Additionally, a dynamic model will be created, incorporating an unglazed transpired solar collector (UTSC). This model will be able to determine the optimal design and operating parameters for the UTSC, thereby enhancing the overall performance of the ASHP system.

4. Conclusions

The performance of the ASHP system of the case study was analysed according to the outdoor air parameters (temperature, relative humidity) and hot water supply temperature. The main conclusions drawn from this research are as follows:

- The ASHP of the case study had the lowest indicators/efficiencies when the external air temperature was about -0.14 °C and RH 95.1%, respectively, the COP value was only 1.49 and the exergy efficiency was 21.2%.
- During a colder day, where the mean external air temperature was -4.23 °C and RH 92.8%, the COP was 1.82, and the exergy efficiency was 26.8%.
- The ratio of air enthalpy and hot water enthalpy used in the analysis helped to estimate the dependence of the exergy efficiency and operating conditions.
- The greater dispersion of the exergy efficiency showed both the change in operating conditions and the performance characteristics of the equipment itself, for example, more frequent freezing of the evaporator surface.

References

- Akbulut, U., Utlu, Z., & Kincay, O. (2016). Exergy, exergoeconomic evaluation of a heat pump-integrated wall heating system. *Energy*, *107*, 502–522. <https://doi.org/10.1016/j.energy.2016.04.050>
- Alva, G., Lin, Y., & Fang, G. (2018). An overview of thermal energy storage systems. *Energy*, *144*, 341–378. <https://doi.org/10.1016/j.energy.2017.12.037>
- Amer, M., & Wang, C. C. (2017). Review of defrosting methods. *Renewable and Sustainable Energy Reviews*, *73*, 53–74. <https://doi.org/10.1016/j.rser.2017.01.120>
- Bonin, J. (2015). *Heat pump planning handbook*. Routledge. <https://doi.org/10.4324/9781315708584>
- Çakir, U., Çomakli, K., Çomakli, Ö., & Karsli, S. (2013). An experimental exergetic comparison of four different heat pump systems working at same conditions: As air to air, air to water, water to water and water to air. *Energy*, *58*, 210–219. <https://doi.org/10.1016/j.energy.2013.06.014>
- Carroll, P., Chesser, M., & Lyons, P. (2020). Air Source Heat Pumps field studies: A systematic literature review. *Renewable and Sustainable Energy Reviews*, *134*, 110275. <https://doi.org/10.1016/j.rser.2020.110275>
- Chen, S. Y. (2019). Use of green building information modeling in the assessment of net zero energy building design. *Journal of Environmental Engineering and Landscape Management*, *27*(3), 174–186. <https://doi.org/10.3846/jeelm.2019.10797>
- Chung, Y., Yoo, J. W., Kim, G. T., & Kim, M. S. (2019). Prediction of the frost growth and performance change of air source heat pump system under various frosting conditions. *Applied Thermal Engineering*, *147*, 410–420. <https://doi.org/10.1016/j.applthermaleng.2018.10.085>
- Dincer, I., & Rosen, M. A. (2015). *Exergy analysis of heating, refrigerating and air conditioning: Methods and applications*. Elsevier.
- Dincer, I., & Abu-Rayash, A. (2020). Sustainability modeling. In *Energy sustainability* (pp. 119–164). Elsevier. <https://doi.org/10.1016/B978-0-12-819556-7.00006-1>
- Dincer, I., & Rosen, M. A. (2013). Exergy analysis of thermal energy storage systems. In *Exergy* (pp. 133–166). <https://doi.org/10.1016/B978-0-08-097089-9.00009-7>
- Dong, X., Tian, Q., & Li, Z. (2017). Energy and exergy analysis of solar integrated air source heat pump for radiant floor heating without water. *Energy and Buildings*, *142*, 128–138. <https://doi.org/10.1016/j.enbuild.2017.03.015>
- European Academies' Science Advisory Council. (2021). *Decarbonisation of buildings: For climate, health and jobs* (EASAC policy report No. 43). https://easac.eu/fileadmin/PDF_s/reports_statements/Decarb_of_Buildings/EASAC_Decarbonisation_of_Buildings_Web_publication030621.pdf
- EurObserv'ER. (2021). *Heat pumps barometer 2021*. <https://www.eurobserv-er.org/heat-pumps-barometer-2021/>
- European Commission. (2019). *The European green deal*. Brussels. <https://eur-lex.europa.eu/legal-content/EN/TXT/?uri=COM%3A2019%3A640%3AFIN>
- García-Gáfaró, C., Escudero-Revilla, C., Flores-Abascal, I., Hidalgo-Betanzos, J. M., & Erkoreka-González, A. (2022). A photovoltaic forced ventilated façade (PV-FVF) as heat source for a heat pump: Assessing its energetical profit in nZEB buildings. *Energy and Buildings*, *261*, 111979. <https://doi.org/10.1016/j.enbuild.2022.111979>
- Gupta, R., & Irving, R. (2013). Development and application of a domestic heat pump model for estimating CO₂ emissions reductions from domestic space heating, hot water and potential cooling demand in the future. *Energy and Buildings*, *60*, 60–74. <https://doi.org/10.1016/j.enbuild.2012.12.037>
- Hwang, J., & Cho, K. (2014). Numerical prediction of frost properties and performance of fin-tube heat exchanger with plain fin under frosting. *International Journal of Refrigeration*, *46*, 59–68. <https://doi.org/10.1016/j.ijrefrig.2014.04.026>
- Kropas, T., Streckienė, G., & Bielskus, J. (2021). Experimental investigation of frost formation influence on an air source heat pump evaporator. *Energies*, *14*(18), 5737. <https://doi.org/10.3390/en14185737>
- Kropas, T., Streckienė, G., Kirsanovs, V., & Džikevičs, M. (2022). Investigation of heat pump efficiency in Baltic States using

- TRNSYS simulation tool. *Environmental and Climate Technologies*, 26(1), 548–560. <https://doi.org/10.2478/rtuect-2022-0042>
- Lepiksaar, K., Kalme, K., Siirde, A., & Volkova, A. (2021). Heat pump use in rural district heating networks in Estonia. *Environmental and Climate Technologies*, 25(1), 786–802. <https://doi.org/10.2478/rtuect-2021-0059>
- Malenković, I. (2012). *Definition of performance figures for solar and heat pump systems* (IEE Technical Report No. 5.1.3). <http://www.estif.org/solarkeymarknew/images/downloads/QAiST/qaist%20d5.1%20tr%205.1.3%20performance%20figures.pdf>
- Ministry of Environment of the Republic of Lithuania. (2022). *Dėl Lietuvos Respublikos aplinkos ministro 2016 m. lapkričio 11 d. įsakymo Nr. D1-754 „Dėl statybos techninio reglamento STR 2.01.02:2016 „Pastatų energinio naudingumo projektavimas ir sertifikavimas“ pakeitimo* (Nr. D1-281). Vilnius.
- Madonna, F., & Bazzocchi, F. (2013). Annual performances of reversible air-to-water heat pumps in small residential buildings. *Energy and Buildings*, 65, 299–309. <https://doi.org/10.1016/j.enbuild.2013.06.016>
- Martinaitis, V. (2007). *Termodinaminė analizė*. Technika. <https://doi.org/10.3846/875-S>
- Martinaitis, V., Streckienė, G., Bagdanavicius, A., & Bielskus, J. (2018). A comparative thermodynamic analysis of air handling units at variable reference temperature. *Applied Thermal Engineering*, 143, 385–395. <https://doi.org/10.1016/j.applthermaleng.2018.07.122>
- Mateu-Royo, C., Navarro-Esbri, J., Mota-Babiloni, A., Molés, F., & Amat-Albuixech, M. (2019). Experimental exergy and energy analysis of a novel high-temperature heat pump with scroll compressor for waste heat recovery. *Applied Energy*, 253, 113504. <https://doi.org/10.1016/j.apenergy.2019.113504>
- Mete Ozturk, M., Doğan, B., & Berrin Erbay, L. (2020). Performance assessment of an air source heat pump water heater from exergy aspect. *Sustainable Energy Technologies and Assessments*, 42, 100809. <https://doi.org/10.1016/j.seta.2020.100809>
- Metrel. (2021). *MD 9272 leakage clamp TRMS meter with power functions* [Apparatus]. <https://www.metrel.si/en/shop/DMM/clamp-meters/md-9272.html>
- MultiMeter/Datalogger EX542 specification*. (2021). https://www.extech-online.com/index.php?main_page=product_info&cPath=78_16_53&products_id=248
- Njoku, H. O., Ekechukwu, O. V., & Onyegegbu, S. O. (2016). Comparison of energy, exergy and entropy generation-based criteria for evaluating stratified thermal store performances. *Energy and Buildings*, 124, 141–152. <https://doi.org/10.1016/j.enbuild.2016.04.062>
- Onset. (n.d.-a). *Temperature/RH smart sensor (S-THB-M002)* [Apparatus]. <https://www.onsetcomp.com/resources/documentation/11427-man-s-thb>
- Onset. (n.d.-b). *12-bit temperature smart sensor (S-TMB-M017)* [Apparatus]. <https://www.onsetcomp.com/products/sensors/s-tmb-m0xx>
- Onset. (2021). *No-lead water flow meter sensor (T-MINOL-130-NL)* [Apparatus]. <https://www.onsetcomp.com/products/sensors/t-minol-130-nl>
- Popiel, C. O., & Wojtkowiak, J. (1998). Simple formulas for thermo-physical properties of liquid water for heat transfer calculations (from 0 °C to 150 °C). *Heat Transfer Engineering*, 19(3), 87–101. <https://doi.org/10.1080/01457639808939929>
- Protective caps for capacitive humidity sensors FHA 646 E1*. (2021). <https://www.priniotakis.gr/catalog2/manuals/Capacitive%20humidity%20sensor,%20protective%20caps.pdf>
- Pyliavskiy, I., Martusenko, I., Molnar, O., Dzyana, H., & Kushniriuk, V. (2021). Modeling ways of improving green economy and environmental protection in the context of governance. *Business: Theory and Practice*, 22(2), 310–317. <https://doi.org/10.3846/btp.2021.13336>
- Rafati Nasr, M., Fauchoux, M., Besant, R. W., & Simonson, C. J. (2014). A review of frosting in air-to-air energy exchangers. *Renewable and Sustainable Energy Reviews*, 30, 538–554. <https://doi.org/10.1016/j.rser.2013.10.038>
- Rimbala, J., Votava, J., & Kyncl, J. (2019). Assessment of energy consumption in the residential building with a heat pump. In *Proceedings of the 2019 20th International Scientific Conference on Electric Power Engineering* (pp. 1–5). IEEE. <https://doi.org/10.1109/EPE.2019.8778066>
- Shao, S., Zhang, H., Fan, X., You, S., Wang, Y., & Wei, S. (2021). Thermodynamic and economic analysis of the air source heat pump system with direct-condensation radiant heating panel. *Energy*, 225, 120195. <https://doi.org/10.1016/j.energy.2021.120195>
- Song, M., Deng, S., Dang, C., Mao, N., & Wang, Z. (2018). Review on improvement for air source heat pump units during frosting and defrosting. *Applied Energy*, 211, 1150–1170. <https://doi.org/10.1016/j.apenergy.2017.12.022>
- Wang, F., Zhao, R., Xu, W., Huang, D., & Qu, Z. (2021). A heater-assisted air source heat pump air conditioner to improve thermal comfort with frost-retarded heating and heat-uninterrupted defrosting. *Energies*, 14(9), 1–13. <https://doi.org/10.3390/en14092646>
- Wang, Y., Ye, Z., Song, Y., Yin, X., & Cao, F. (2020). Energy, exergy, economic and environmental analysis of refrigerant charge in air source transcritical carbon dioxide heat pump water heater. *Energy Conversion and Management*, 223, 113209. <https://doi.org/10.1016/j.enconman.2020.113209>
- Willem, H., Lin, Y., & Lekov, A. (2017). Review of energy efficiency and system performance of residential heat pump water heaters. *Energy and Buildings*, 143, 191–201. <https://doi.org/10.1016/j.enbuild.2017.02.023>
- Witkowska, A., Krawczyk, D. A., & Rodero, A. (2021). Analysis of the heat pump market in Europe with a special regard to France, Spain, Poland and Lithuania. *Environmental and Climate Technologies*, 25(1), 840–852. <https://doi.org/10.2478/rtuect-2021-0063>